

Fig. S1. Line scans of cell wall staining reveals unique patterns of chitin and β -1,3-glucan deposition in core septin null mutants. (A) Line scan profiles (Left column) of aniline blue staining patterns, corresponding to the red arrows drawn through the hyphal tips of WT and $\Delta aspB^{cdc3}$ (Right column). (B) Line scan profiles (Left column) of calcofluor white staining patterns, corresponding to the red arrows drawn through the hyphal tips of WT and $\Delta aspB^{cdc3}$ (Right column). Asterisk in Panel A line scan profile denotes saturation of fluorescence signal.

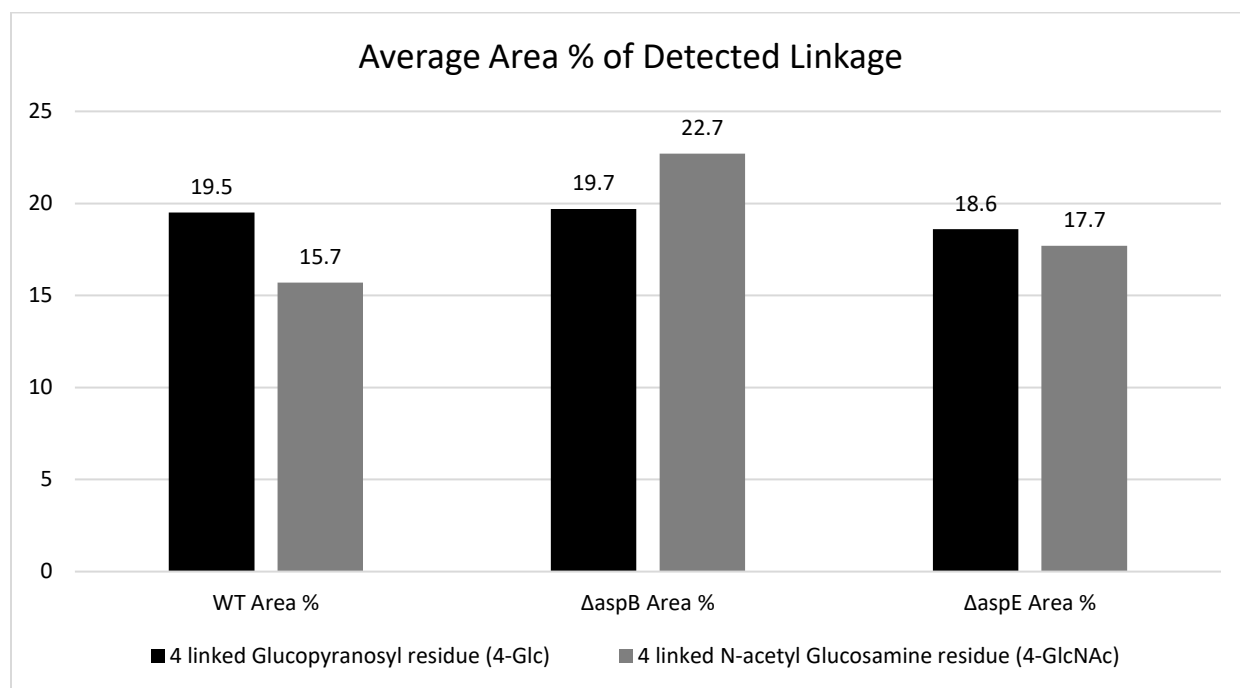


Fig. S2. Cell wall glycosyl linkage analysis shows increased chitin content in $\Delta aspB^{cdc3}$ septin null mutant. Results of cell wall polysaccharide glycosyl linkage analysis using GC MS/MS showing the average area (%) of detected linkages of 4-linked glucose and 4-linked N-acetyl glucosamine. Two independent biological replicates gave similar results. A representative data set is shown. Samples: WT, $\Delta aspB^{cdc3}$, and $\Delta aspE$.

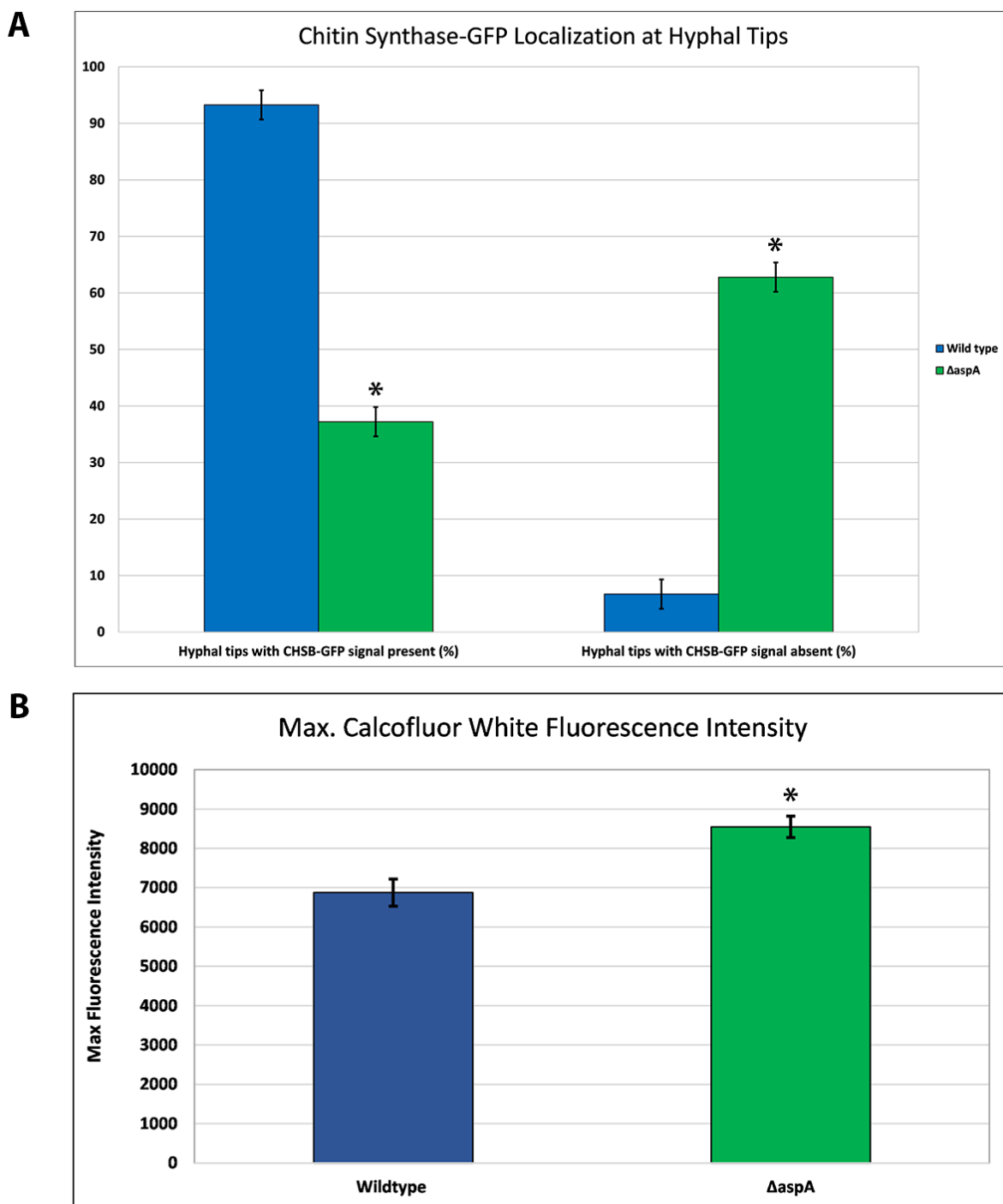


Fig. S3. Quantification of chitin synthase B-GFP and CFW fluorescence signal. (A) Quantification of percentage (%) of hyphal branch tips with chitin synthase B-GFP present vs. absent by line scans in WT and $\Delta\text{aspA}^{cdc11}$. Mean values shown for line scans of ≥ 85 hyphal branches over two independent biological replicates. Asterisks indicate different standard error of the mean between sample sets. (B) Quantification of maximum fluorescence intensity by line scans of CFW stained WT and $\Delta\text{aspA}^{cdc11}$

hyphae (subapical region). Mean values shown for line scans of ≥ 65 hyphal branches over two independent biological replicates. Asterisks indicate different standard error of the mean between sample sets and statistically different values by two-tailed Ttest ($p < 0.05$) ($N=50$).

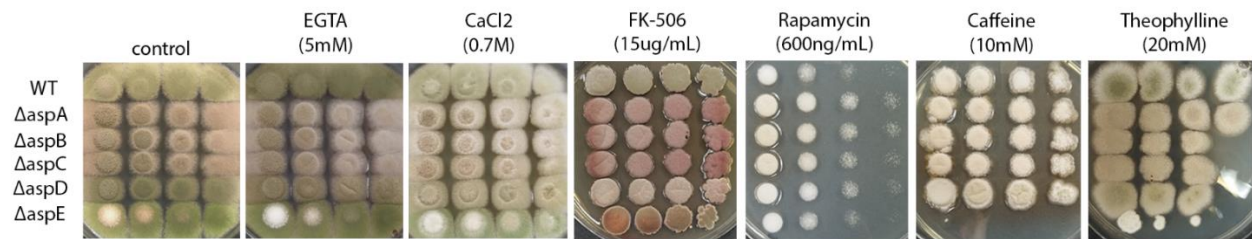


Fig. S4. Core septin null mutants are not sensitive to treatments which disrupt the Ca^{2+} /Calcineurin or TOR pathways. AspE is hypersensitive to treatments which disrupt the TOR pathway. WT and septin null mutants $\Delta\text{aspA}^{cdc11}$, ΔaspB^{cdc3} , $\Delta\text{aspC}^{cdc12}$, $\Delta\text{aspD}^{cdc10}$, and ΔaspE were tested for sensitivity by spotting decreasing spore concentrations on complete media plates with or without Calcium/Calcineurin pathway-disturbing agents (EGTA, CaCl_2 , and FK-506) or Target of Rapamycin (TOR) pathway-disturbing agents (Rapamycin, caffeine, and theophylline). Differences in colony color result from changes in spore production, spore pigment, and production of secondary metabolites under stress. Spore concentrations were [1^7 conidia/mL – 10^4 conidia/mL] for all assays in figure. N=3

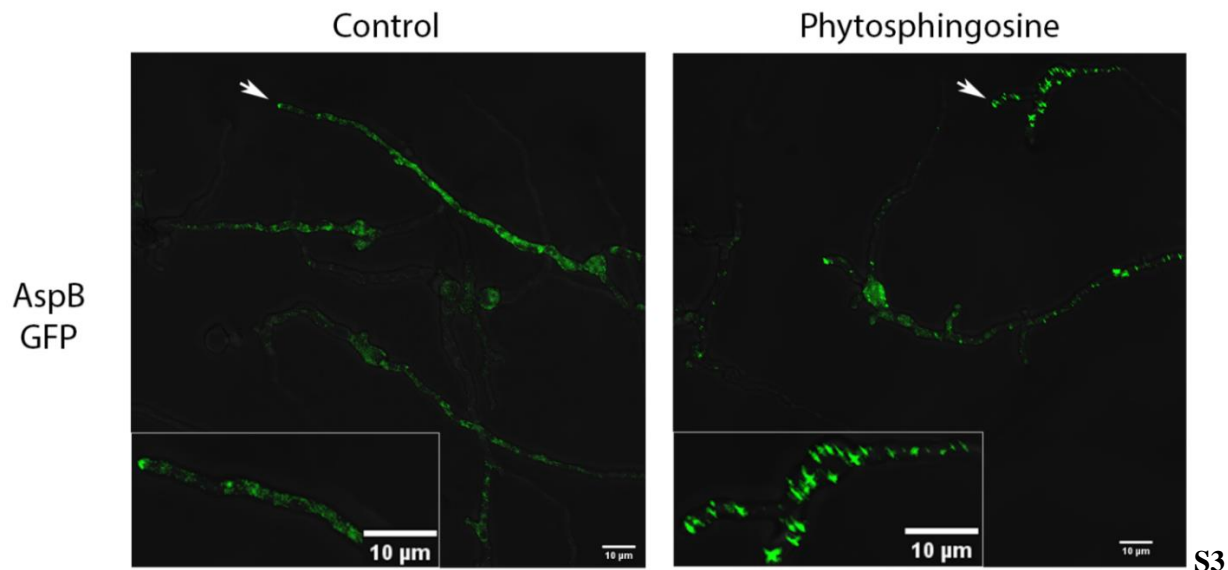


Fig. S5. Septin AspB^{Cdc3}-GFP localization disrupted by sphingolipid biosynthesis intermediate phytosphingosine. AspB^{Cdc3}-GFP strain incubated in liquid media for approximately 16h and imaged 180 minutes after replacing with fresh media containing sphingolipid biosynthesis-inhibiting agents. Representative images are shown from three independent biological replicates, with ≥ 100 cells observed. (Left Panel) AspB-GFP in vehicle control treatments and (Right Panel) phytosphingosine (15 μM) treatment. Enlarged section of micrographs from each picture to better visualize pattern of fluorescence. White arrows denote hyphae which are highlighted in enlarged images. Imaging conducted with Deltavision I deconvolution inverted fluorescence microscope. Scale bars = 10 μm. N=3

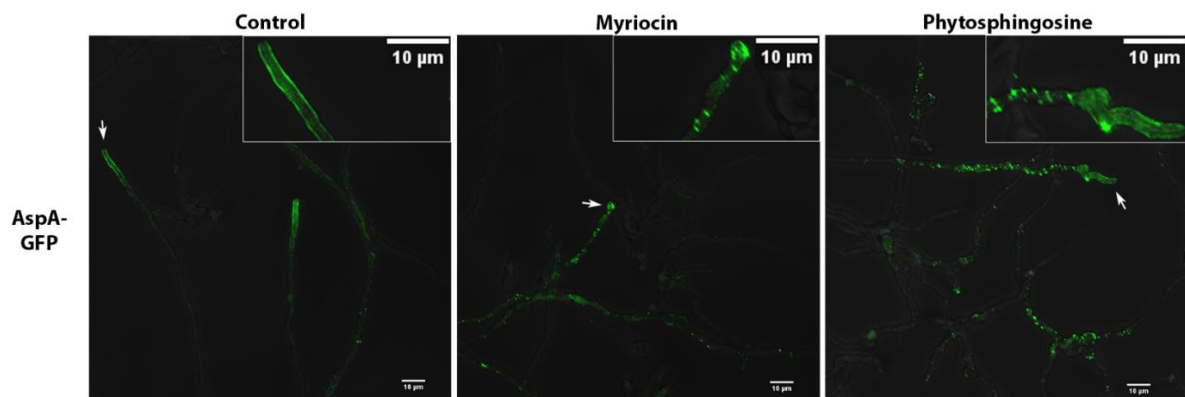


Fig. S6. Septin AspA^{Cdc11}-GFP localization disrupted by sphingolipid biosynthesis inhibitors. AspA^{Cdc11}-GFP strain incubated in liquid media for approximately 16h and imaged 180 minutes after replacing with fresh media containing sphingolipid biosynthesis-inhibiting agents. Representative images are shown from three independent biological replicates, with ≥ 100 cells observed. (Left Panel) AspA-GFP in vehicle control treatment, (Middle Panel) Myriocin (17.5 μg/mL) and (Right Panel) phytosphingosine (15 μM) treatment. Enlarged section of micrographs from each picture to better visualize pattern of fluorescence signal. White arrows denote hyphae which are highlighted in enlarged images. Imaging conducted with Deltavision I deconvolution inverted fluorescence microscope. Scale bars = 10 μm . N=3

Table S1. List of fungal strains used in this study.

Strain Number	Genotype	Source
FGSC A850 (WT)	biA1; _argB::trpC_B; methG1; veA1; trpC801	FGSC
ASH5 (Δ aspA)	aspA::argB2 biA1 argB::trpC_B methG1 veA1 trpC801	Lindsey and Momany, 2010
AYR32 (Δ aspB)	aspB::AfpyrG; pyroA4; argB2	Hernandez-Rodriguez et al., 2012
ARL161 (Δ aspC)	aspC::AfpyrG pyrG89 biA1 argB::trpC_B methG1 veA1 trpC801	Lindsey and Momany, 2010
AKK3 (Δ aspD)	aspD::AfpyrG; pyroA4; argB2	Hernandez-Rodriguez et al., 2014
ASH41 (Δ aspE)	aspE::AfpyrG; riboB2	Hernandez-Rodriguez et al., 2012
ANID_05666 (Δ mpkA)	pyrG89; argB2; Δ nkuA(ku70)::argB; Δ mpkA::pyrG; pyroA	CP De Souza et al., 2013
AAM016 (Δ mpkA Δ aspB)	aspB::AfpyrG; pyroA4; argB2 + pyrG89; argB2; Δ nkuA(ku70)::argB; Δ mpkA::pyrG; pyroA	This study
AAM017 (Δ mpkA Δ aspB)	aspB::AfpyrG; pyroA4; argB2+ pyrG89; argB2; Δ nkuA(ku70)::argB; Δ mpkA::pyrG; pyroA	This study

AAM019 (ΔmpkAΔaspE)	aspE::AfpyrG; riboB2+ pyrG89;argB2;ΔnkuA(ku70)::argB;ΔmpkA::pyrG;pyroA	This study
AAM020 (ΔmpkAΔaspE)	aspE::AfpyrG; riboB2+ pyrG89; argB2;ΔnkuA(ku70)::argB;ΔmpkA::pyrG;pyroA	This study
ARL141	<i>aspA-GFP-AfpyrG pyrG89 biA1 argB::trpC_B methG1 veA1 trpC801</i>	Lindsey and Momany, 2010
EB-5	<i>biA1 pyrG89 argB2 pyroA4 wa3 ΔchsB::pyr-4-alcA(p)-chsB argB::chsB(p)-egfp-chsB</i>	Fukuda et al., 2009
AAM022	<i>aspA::argB2 biA1 pyrG89 argB2 wa3 ΔchsB::pyr-4-alcA(p)-chsB argB::chsB(p)-egfp-chsB</i>	This study

Table S2. List of primers and sequences used in this study.

Primer Name	Primer Sequence
PyrG-Af-R'	5'-CAG AGC CCA CAG AGC GCC TTG AG-3'
AspB-KO-F'	5'-GGT CAT TCC TGG TGT GAC AGT ACC-3'
AspE-KO-F'	5'-GAT CCA AAT TCC AGG TTC GAT GAC-3'
MpkA-806-F'	5'-ATC CTA GAC TCG ACG CCT CA-3'
MpkA-3779-R'	5'-ACA AAA ACC CCA TCG TCC GA-3'
AspA-KO-F'	5'-TAG ATC AAG CTC CGC CGG AA-3'
AspA-KO-R'	5'-TGA CTC CAG CGA CGA TGA GT-3'